



LAWRENCE
LIVERMORE
NATIONAL
LABORATORY

Time-resolved Soft X-Ray Imaging (SXRI) diagnostic for use at the NIF and OMEGA lasers

M.B. Schneider, J.P. Holder, D.L. James, H.C. Bruns, J.R. Celeste, S. Compton, R.L. Costa, A.D. Ellis, J.A. Emig, D. Hargrove, D.H. Kalantar, B.J. MacGowan, G.D. Power, C. Sorce, V. Rekow, K. Widmann, B.K. Young, P.E. Young, O.F. Garcia, J. McKenney, M. Haugh, F. Goldin, L.P. MacNeil, K. Cone

May 5, 2006

16th Topical Conf. on High Temperature Plasma Diagnostics,
Williamsburg, VA, United States
May 7, 2006 through May 11, 2006

Disclaimer

This document was prepared as an account of work sponsored by an agency of the United States Government. Neither the United States Government nor the University of California nor any of their employees, makes any warranty, express or implied, or assumes any legal liability or responsibility for the accuracy, completeness, or usefulness of any information, apparatus, product, or process disclosed, or represents that its use would not infringe privately owned rights. Reference herein to any specific commercial product, process, or service by trade name, trademark, manufacturer, or otherwise, does not necessarily constitute or imply its endorsement, recommendation, or favoring by the United States Government or the University of California. The views and opinions of authors expressed herein do not necessarily state or reflect those of the United States Government or the University of California, and shall not be used for advertising or product endorsement purposes.

**Time-resolved Soft X-Ray Imaging (SXRI) diagnostic for use at the NIF and
OMEGA lasers**

M.B. Schneider, J.P. Holder, D.L. James, H. C. Bruns, J.R. Celeste, S. Compton, R.L.
Costa, A.D. Ellis, J.A. Emig, D. Hargrove, D.H. Kalantar, B.J. MacGowan, G.D. Power,
C. Sorce, V. Rekow, K. Widmann, B.K. Young, P.E. Young

Lawrence Livermore National Laboratory

Livermore, CA 94550

O.F. Garcia, J. McKenney

Sandia National Laboratories

Albuquerque, NM 87185

M. Haugh, F. Goldin, L.P. MacNeil

Bechtel Nevada

Livermore, CA 94550

K. Cone

University of California at Davis

Davis, CA 95616

Abstract

The soft x-ray imager (SXRI) built for the first experiments at the National Ignition Facility (NIF) has four soft x-ray channels and one hard x-ray channel. The SXRI is a snout that mounts to a four strip gated imager. This produces four soft x-ray images per strip, which can be separated in time by ~ 60 psec. Each soft x-ray channel consists of a mirror plus a filter. The diagnostic was used to study x-ray burnthrough of hot hohlraum targets at the NIF and OMEGA lasers. The SXRI snout design and issues involved in selecting the desired soft x-ray channels are discussed.

I. Introduction

Two-dimensional time-resolved images of thermal x-rays have been extensively used[1] in hohlraum experiments at the Omega[2] and Nova[3] lasers to study diagnostic hole closure, spatial profiles of laser entrance holes, and to monitor thermal x-ray burnthrough. The x-ray burnthrough technique is a method of measuring the radiation temperature inside a hohlraum.[4-6] The x-radiation heats the hohlraum wall, and the heat diffuses through the wall in a Marshak heat wave[4]. The time it takes to heat a wall of known thickness is the x-ray burnthrough time.

Burnthrough time is traditionally measured with a soft x-ray snout on an x-ray streak camera looking at a thin patch of wall material of known thickness. The patch covers a diagnostic slit in the hohlraum. The patch technique does not work for very small targets such as Hot Hohlraums[7-9]. These small targets (designed to reach high radiation temperatures) are $\sim 800\mu\text{m}$ in diameter or smaller. For the x-ray burnthrough experiments, these targets have uniformly thin walls (no patches). Previous experiments[10] show that the burnthrough pattern is not uniform in these small targets. This means two-dimensional time-resolved images are required to interpret the streak-camera data. In addition, the x-ray streak camera data recorded on these shots is compromised by a high hard x-ray background and EMP [11]. For these reasons, the soft x-ray imager (SXRI) diagnostic was built to provide sixteen soft x-ray images of x-ray burnthrough separated by $\sim 60\text{psec}$ in time. Figure 1 shows data from the SXRI.

II. Description of the SXRI

SXRI is modeled after the soft x-ray imager (SXR) snout[1] which has two soft x-ray channels and one hard x-ray channel and is used extensively at OMEGA and elsewhere. SXRI has four soft x-ray channels, each consisting of a grazing angle-of-incidence mirror and a filter, and one (filtered) hard x-ray (straight-through) channel. Each soft x-ray channel passes a band of soft x-rays, the lowest energy determined by the filter and the high energy cut-off is set by the mirror. Figure 2 shows a schematic diagram of SXRI. It is mated to an x-ray framing camera, such as the FXI (Flexible X-ray Imager)[12] which has four microchannel plate (MCP) striplines. An image from each of the four soft x-ray channels is produced along a single ~34mm long MCP stripline. The optical gate width is ~85psec for a 200psec pulse forming module[12]. The images are separated in space by 8.4mm along the striplines. Since a voltage pulse travels along the stripline at about half the velocity of light[13], the images are separated by ~60psec in time. Each stripline has one image from each soft x-ray channel, and one straight-through hard x-ray image centered between the two central soft x-ray images. By suitably selecting the trigger time for each stripline, the 16 soft x-ray images can produce a continuous time-record for ~900psec.

The SXRI snout uses a combination of 2° angle-of-incidence and a set of 3° angle-of-incidence mirrors. Figure 3 shows the SXRI as designed and built. The 2° mirrors are centered 435 mm from target chamber center (TCC) and are tilted 0.6°

towards TCC with respect to the centerline of the snout. The 3° mirrors are centered 540 mm from TCC and are tilted 2.2° towards TCC. The distance from TCC to the MCP is fixed at 762mm (30"). Magnification is determined by the location of the pinholes. The SXRI can have magnifications from 1.2x to 8x.

The SXRI mirrors are $\sim 1500\text{\AA}$ metal coated onto a BK-7 substrate. The mirror is 3.000" in length, 0.500" in width and 0.850" in height. Machined into the long sides of the BK-7 substrate is a 0.040" x 0.040" groove. A small "L" shaped clamp fits into the groove and attaches the mirrors to a mirror-mounting block. The mirror-mounting block has tapped holes in it for the "L" clamp and through holes for mounting to a kinematic base using 6-32 screws. The kinematic base incorporates the mirror tilt machined into its surface. The mirror assembly (mirror plus holder plus kinematic base) fits into position in the SXRI body via a spring-loaded kinematic assembly. Except for shielding, the SXRI is made of aluminum with stainless steel fasteners (i.e., no glue, to meet NIF's vacuum requirements). The SXRI snout is aligned in an offline alignment station. If necessary, shims are inserted between the BK-7 mirror and mirror-mounting block. The mirror assembly can be removed and replaced but the alignment is preserved.

The MCP is well shielded from hard x-rays and stray light. The pinhole assembly consists of (in order, from TCC towards the detector): 0.011" thick tantalum collimator, 0.010" thick tantalum pinhole substrate, 0.011" thick tungsten collimator, and 0.011" thick tantalum collimator. The collimators have $300\mu\text{m}$ diameter holes whereas the pinholes are $25\mu\text{m}$ diameter holes. All pinholes are checked before use. There is a

0.125" thick light baffle with 0.110" diameter holes placed in the plane where the nosecone attaches to the SXRI body. Finally, there is a 0.75" thick heavymet (machineable tungsten) shield after the mirrors, approximately in the plane where the x-rays from all the images cross. These are shown in Figure 3.

The filter assembly consists of thin filters sandwiched between two 0.020" thick stainless steel frames(see Section III). It is placed in the filter position of the Unimount adaptor which is the metal plate that is the interface between a framing camera snout and the framing camera. The filters are thus ~22mm from the MCP.

Table I gives the field-of-view (FOV) for different magnifications. The vertical FOV is the distance a point source near TCC can move such that its light goes through the pinhole and falls on the 6mm wide MCP stripline. The horizontal FOV is 80% of the distance a point source can be moved near TCC such that its light goes through the pinhole and hits both mirrors. If the magnification times the horizontal FOV is equal or less than ~4mm, there is room on the MCP between the two 2° images for the straight-through hard x-ray channel.

Figure 4 gives the spatial resolution versus x-ray energy for SXRI assuming 25 μ m diameter pinholes and 70 μ m resolution for the MCP.

III. Filters

The x-ray bandpass of the soft x-ray channels are determined by the mirrors and filters. For the x-ray burnthrough application, it is desirable for the four channels to pass the same spectral band. Because the MCP has a dynamic range of only 300[13], it is desirable for the images from the four channels to have approximately the same maximum intensity. The optical gain of the MCP decreases along the strip, due to ohmic losses [13]. If the strip is not impedance matched, there is also a voltage reflection which adds gain at the end of the strip and changes the timing of the fourth image. This reflection effect varies greatly among cameras. Figure 5 illustrates this.

Initially, filters were designed[14] to compensate for the loss of MCP gain, assuming no reflection. To protect the MCP against filter breakage due to pressure bursts from pump-down or venting, it was required to mount the filters on a plastic substrate. Figure 6 shows the initial filter design using 3° Ge mirrors and 2° Al mirrors. The filters were Ni and Co layers coated onto $0.75\mu\text{m}$ thick parylene-N substrate. Several variations of this design (parylene-N, polypropylene, Fe and Ni) were tried. All produced results similar to that shown in Figure 6b: the filters on plastic wrinkled as soon as they became free-standing. We believe this is due to the mismatch between expansion of plastic and the relatively thick metal coating. We recommend using silicon nitride (Si_3N_4) instead of plastic. This is strong, thin, and solid. The wrinkled filters were never used.

The filter configuration that was used is shown in Figure 7. Preliminary results

indicated the presence of a reflection in the MCP gain, so the filters were made symmetric. The filters consist of thin layers of aluminum (2000Å for 3° mirrors and 4000Å for 2° mirrors) coated onto ~0.75µm thick polypropylene. These filters did not wrinkle because the aluminum was so thin and better matched to the plastic. The mirrors are 3° germanium and 2° aluminum. The bandpass is ~500-800eV.

There is a preliminary calibration of the throughput of the mirrors and filters using a monochromatic Henke source. Figure 7b shows the predicted throughput based on the calibration results..

IV Results and future

The SXRI was operated with magnification 3X at OMEGA and NIF. Figure 1 shows sample data showing soft x-ray burnthrough from 600µm micron diameter hohlraums with 3.5µm thick Au wall at OMEGA[10]. The filter on the central hard x-ray channel was 100µm-thick aluminum.

The SXRI may be configured to detect four different soft x-ray energies and thus monitor hohlraum diagnostic or laser entrance hole closure as a function of time and x-ray energy. The development of a better substrate for thin filters is crucial to this application.

Acknowledgements

We thank the NIF and OMEGA staff for their excellent work. Work performed under the auspices of the U.S. Department of Energy by the Lawrence Livermore National Laboratory under Contract No. W-7405-ENG-48 and grant number DE-FG52-2005NA26017 (NLUF).

1. F. Ze, R. L. Kauffman, J. D. Kilkenny, J. Wielwald, P. M. Bell, R. Hanks, J. Stewart, D. Dean, J. Bower, and R. Wallace, *Rev. Sci. Instrum.* **63** (10), 5124 (1992).
2. J. M. Soures et al, *Phys. Plasmas* **3**, 2108, (1996); T. R. Boehly et al, *Opt. Commun.* **133**, 495 (1997).
3. J. Kilkenny, *Rev. Sci. Instrum.* **63**, 4688 (1992).
4. J. Hammer and M. Rosen, *Phys. Plasmas* **10**, 1829, (2003).
5. T.J. Orzechowski, M.D. Rosen, H.N. Kornblum, J.L. Porter, L.J. Suter, A.R.Thiessen, and R. J. Wallace, *Phys. Rev. Lett.* **77** (1996) 3545.
6. R.E. Olson, R.J. Leeper, A. Nobile, et al., *Phys. Plasmas* **11** 2778 (2004).
7. D.E. Hinkel, M.B. Schneider, B.K. Young, A.B. Langdon, E.A. Williams, M.D. Rosen, and L.J. Suter, *Phys. Rev. Lett.* **96** 195001 (2006).
8. M.B. Schneider, D.E. Hinkel, O.L. Landen, et al, "Plasma filling in reduced-scale hohlraums irradiated with multiple beam cones", submitted to *Physics Plasmas* (2006).

9. D. E. Hinkel, M. B. Schneider, et al., *Phys. Plasmas*, **12**, 056305, (2005).
10. M. B. Schneider, D. E. Hinkel, B. K. Young, J.P. Holder, A.B. Langdon, H.A. Baldis, et al., "X-ray flux and x-ray burnthrough experiments on reduced-scale targets at the NIF and OMEGA lasers "in Proceedings of the Fourth International Conference on Inertial Fusion Sciences and Applications, Biarritz, France, 2005 (*to be published*)
11. M.B. Schneider, C. Sorce, K. Loughman, J. Emig, C. Bruns, C. Back, P.M. Bell, S. Compton, D. Hargrove, J.P. Holder, O.L. Landen, T.S. Perry, R. Shepherd, and B.K. Young, *Rev. Sci. Instrum.*, **75**, 4040 (2004).
12. K. S. Budil, T. S. Perry, P.M. Bell, J.D. Hares, P. L. Miller, T.A. Peyser, R. Wallace, H. Louis, and D. E. Smith, *Rev. Sci. Instrum.* **67** 485 (1996).
13. O. L. Landen, P. M. Bell, J. A. Oertel, J. J. Satariano, and D. K. Bradley, *Photonics, and Videography '93*, **SPIE Vol. 2002** (SPIE, Bellingham WA, 1993), p. 2.
14. B.L. Henke, E.M. Gullikson, and J.C. Davis, *Atomic Data and Nuclear Data Tables* **54** no.2, 181-342 (July 1993).

Figure Captions

FIG. 1. SXRI film data from Omega showing time progression of x-ray burnthrough. The views of the target are sketched around the data images. Photos of the target are shown above the film data. The hard x-ray channel has a pinhole image of the target; the images in the mirror channels are flipped horizontally from the pinhole image. The dashed vertical lines show the footprint of the 4mil-thick Al filter used for the hard x-ray channel. The strips are fired every 300 psec. Along a strip, the time between soft x-ray images is ~60 psec. A timing fiducial beam hits the back wall at 1 nsec (bottom strip, 2°L image)

FIG. 2. Concept of the SXRI showing its four soft x-ray mirror+filter channels, its hard x-ray straight-through filter channel, and the four strip microchannel plate (MCP) x-ray framing camera. The tilt of mirrors towards TCC is exaggerated; the true tilts are 0.6° (2° mirrors) and 2.2° (3° mirrors).

FIG. 3. SXRI as (a) designed and (b) built. Magnification can be changed from 1.2X to 8X by placing slits at appropriate distance from TCC (that is, by changing the nosecone).

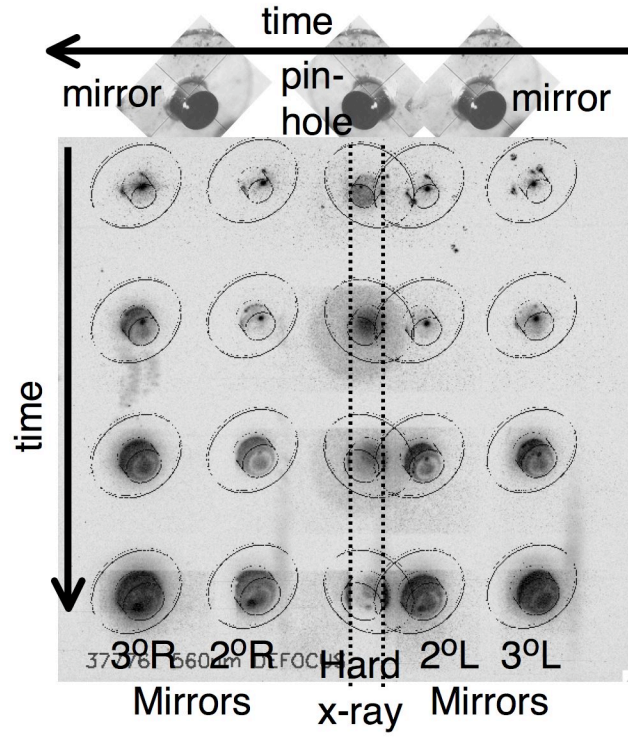
Table I: Field of View vs. Magnification.

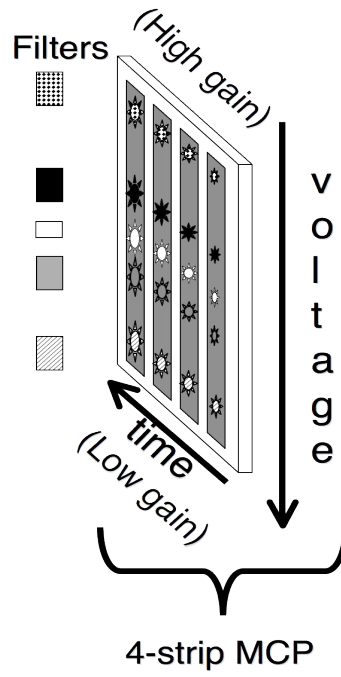
FIG. 4. SXRI Resolution at target plane for 25um pinholes and 70µm-resolution MCP

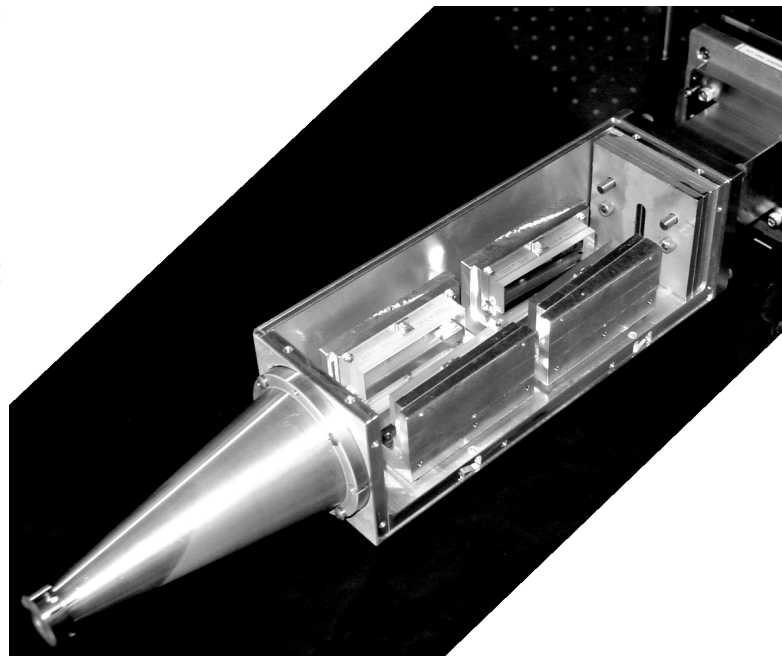
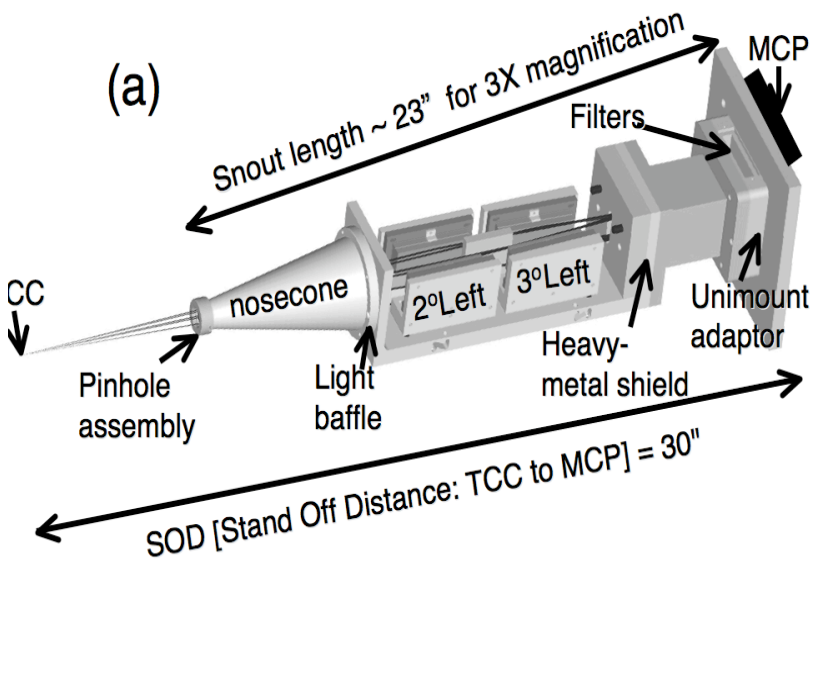
FIG. 5. Measured optical gain vs distance along channel plate strip. The reflection at 30mm varies greatly between framing cameras.

FIG. 6. (a) Filters can be designed to compensate for variation of optical gain along MCP. (b) 0.020"-thick stainless steel filter frame and a filter. A filter made up of a few thousand angstroms of nickel, cobalt, and/or iron on a ~ 0.5 to $1\mu\text{m}$ -thick plastic substrate wrinkled as soon as the filter became free-standing. These filters were never used.

FIG. 7. (a) Construction of filters that are in use and (b) approximate throughput of 2° and 3° channels based on preliminary calibrations with Henke source.

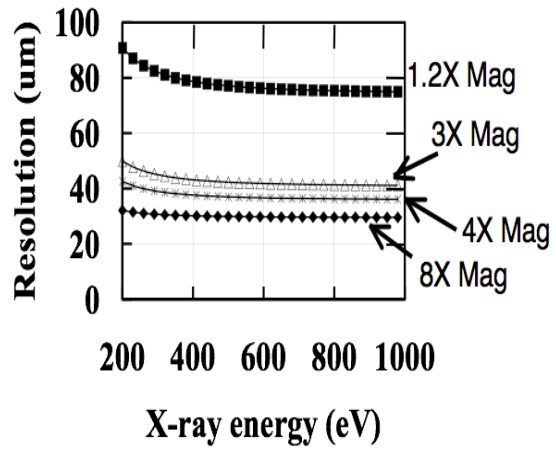


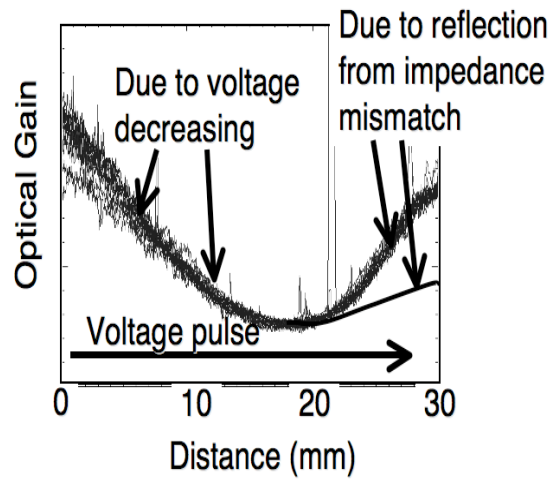


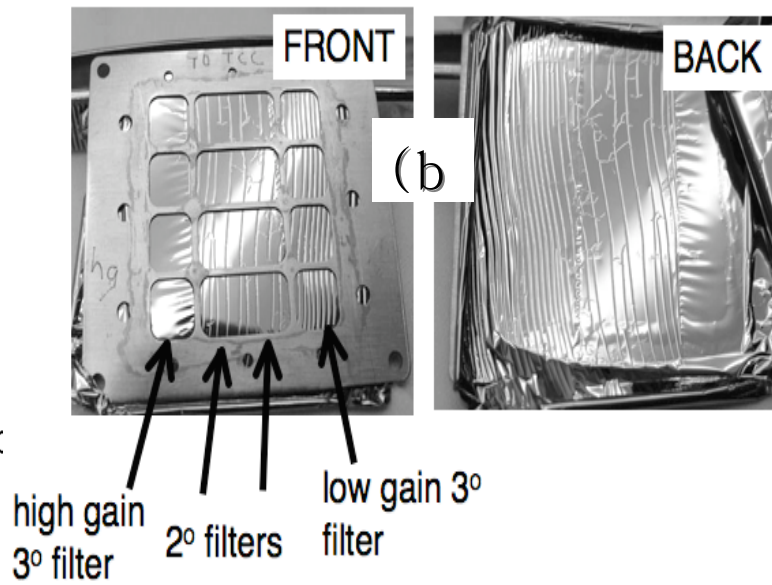
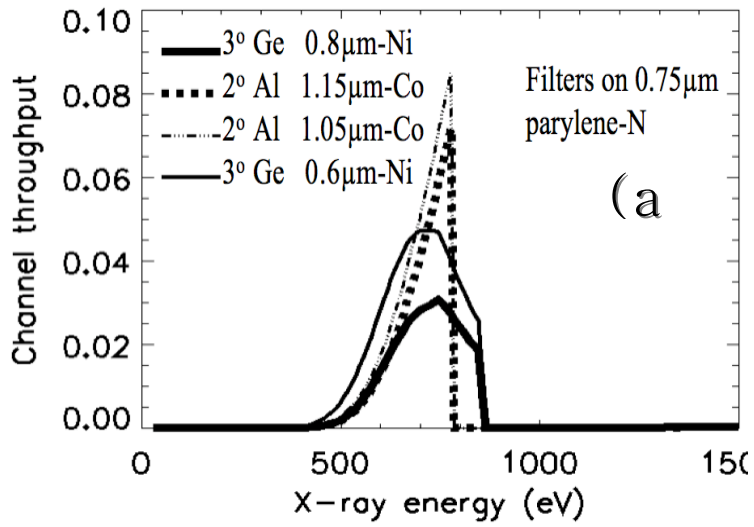


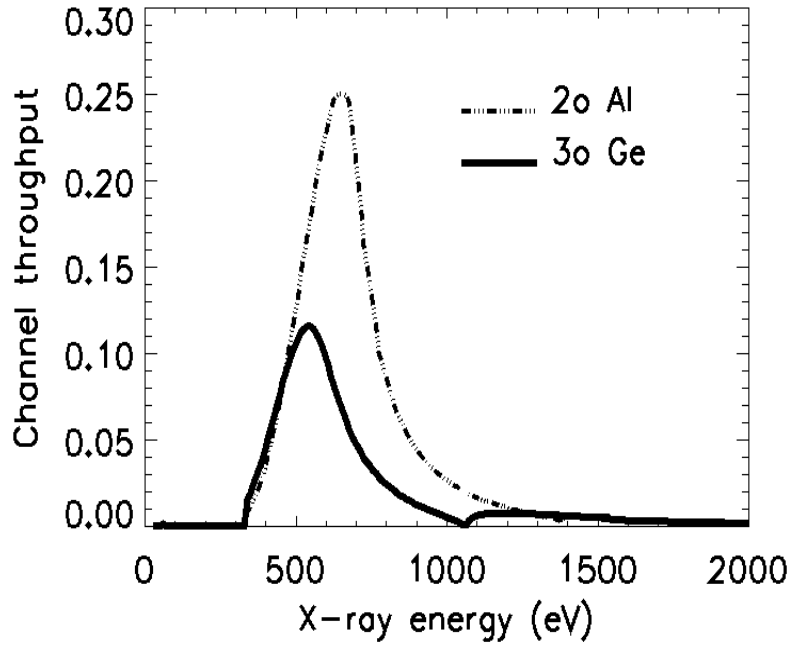
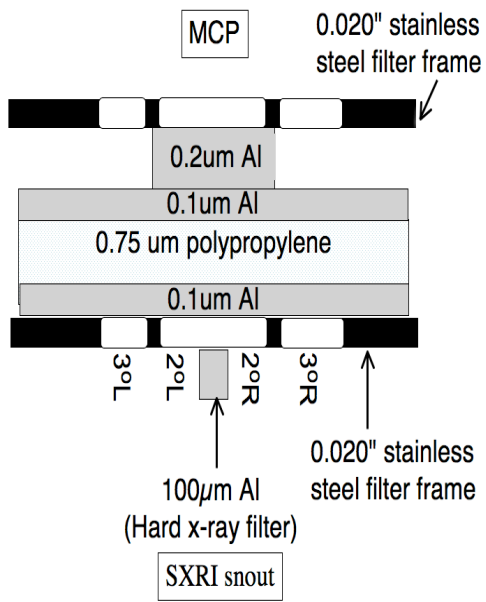
Figure

<u>Mag</u>	<u>FOV (mm)</u>	
	<u>Horizontal</u>	<u>Vertical</u>
1.2	4.8	5
3	1.4	2
4	1.0	1.5
8	0.5	0.75









Fig